

## **DEVELOPMENT OF A WIDEBAND HIGHLY EFFICIENT GAN VMCD VHF/UHF POWER AMPLIFIER**

**S. Lin and A. E. Fathy**

Min H. Kao Department of Electrical Engineering  
and Computer Science  
University of Tennessee  
Knoxville, TN 37996, USA

**Abstract**—A 50 to 550 MHz wideband gallium nitride (GaN) HEMT power amplifier with over 43 dBm output power and 63% drain efficiency has been successfully developed. The demonstrated wideband power amplifier utilizes two GaN HEMTs and operates in a push-pull voltage mode Class D (VMCD). The design is based on a large signal simulation to optimize the power amplifier's output power and efficiency. To assure a wideband operation, a coaxial line impedance transformer has been used as part of the input matching network; meanwhile, a wideband a 1:1 ferrite loaded balun and low pass filters are utilized on the amplifier's output side instead of the conventional serial harmonic termination.

### **1. INTRODUCTION**

There is an increasing demand for high-power wideband RF amplifiers for various applications like wireless and radar applications [1]. Hence, as a variety of power amplifiers (PA) can be typically considered for the transmitter, it is important to investigate the impact of the selection of the PA class of operation on transmitter's overall performance [2–6]. PAs, when their active devices operate as current-sources, are known as conventional linear-mode power amplifiers. PAs, when their active devices operate as switches, are known to theoretically achieve 100% efficiency. These are called switching mode power amplifiers (SMPAs). A comparison between the various SMPAs (Class D, E and F though S) and the conventional linear-mode PAs (Class A, AB, B and C) shows

---

*Received 23 November 2010, Accepted 30 December 2010, Scheduled 23 January 2011*  
Corresponding author: Song Lin (songlin.silva@gmail.com).

that the efficiency of the SMPAs is higher in theory especially when the multi-harmonic load termination is available. Besides having a higher efficiency, SMPAs are also less susceptible to circuit parameter variations. Additional advantages include lower thermal stress on the utilized transistors than the thermal stress generated in a linear-mode PA operation.

“Class D” amplifiers were first discussed by Baxandall [7]. After Baxandall, multiple variations/modifications of Class D power amplifier with noticeably improved performances [8–12] have been lately proposed, however the Class D power amplifier have not been fully researched yet, especially for wideband applications. Efficiencies over 75% have been demonstrated for narrow band or low frequency operation [10], however, it becomes more challenging to exceed 60–65% over decade bandwidth. In this paper, the goal is to confront the challenge of achieving high power, high efficiency over wideband operation. The designed wideband PA uses two GaN HEMTs operating in a push-pull voltage-mode Class D topology, which is driven in such a way to alternately switch the GaN HEMTs ON and OFF; thus acting like a two-pole switch. The almost rectangular wave output voltage is applied to harmonic filters, which contain low pass filters to suppress the harmonics of the rectangular waveform, resulting in wideband amplification with a sinusoidal output. Here, the VMCD circuitry with simulation and experimental results will be presented.

## 2. BASIC CONCEPT OF A CLASS D PA

Traditionally, there are two typical types of Class D PAs. Namely, a transformer coupled voltage-mode Class D (VMCD) and a transformer coupled current-mode Class D (CMCD). The two configurations are shown in Figure 1. These circuits are comprised of two switching devices working under push-pull mode, a resonant RLC tank circuit, an input balun transformer, and an output balun transformer. The VMCD has a constant center-tap voltage  $V_{dd}$  with a capacitor and a series RLC tank. The CMCD has a constant center tap current  $I_{dd}$  with an RF choke and a shunt RLC tank. Subsequently, the VMCD can have a rectangular drain voltage with a half-sine drain current and the CMCD can have a rectangular drain current with a half-sine drain voltage, as shown in Figure 2.

## 3. DEVICE SELECTION FOR CLASS D PA

Ideally, a Class D PA can achieve 100% drain efficiency. However, in any practical circuit, the parasitic of the device, for example,  $C_{ds}$

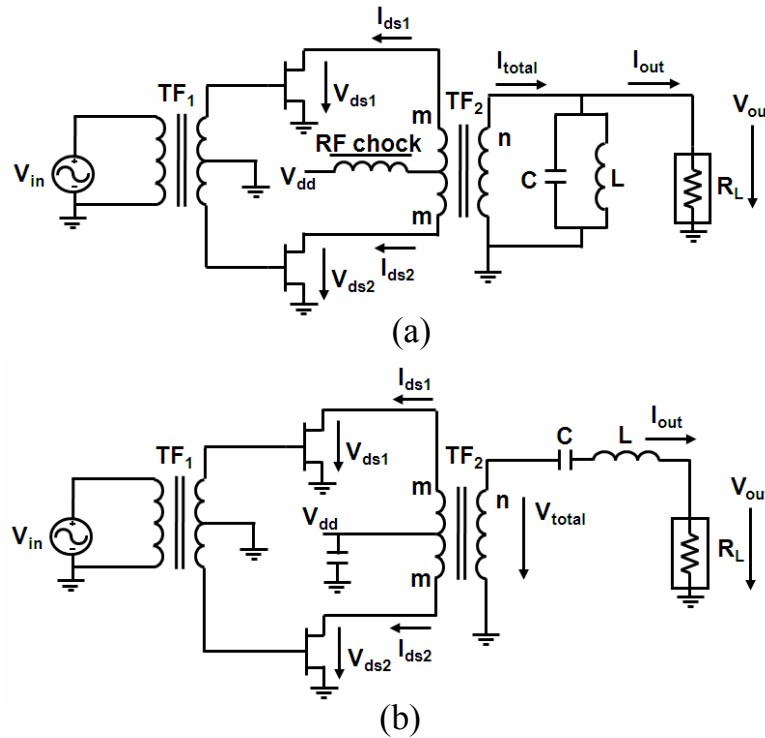


Figure 1. Class D PA configurations: (a) CMCD; (b) VMCD.

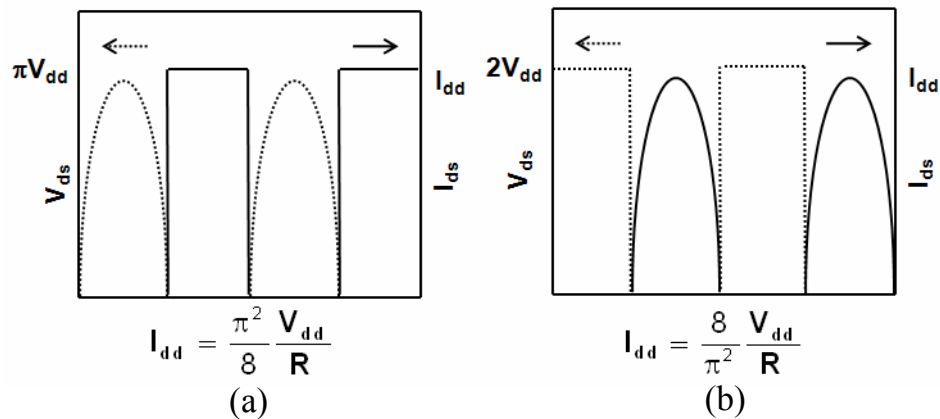


Figure 2. Class D PA transient waveforms: (a) CMCD; (b) VMCD.

and the lead inductance,  $L$ , can cause losses on the order of  $0.5C_{ds}V^2$  and  $0.5LI^2$  respectively, due to their charging-discharging processes. These losses cause a significant drop in drain efficiency. At the same time, additional factors related to the device parameters can cause further efficiency degradation [13]. For example, the saturation voltage of the transistor ( $V_{DSsat}$ ), and the  $ON$ -resistor of the transistor ( $R_{ON}$ ) should have low values. Additionally, in order to have a

device working as a switch and generating a rectangular wave, its gain cut-off frequency ( $f_T$ ) should be at least 10 times higher than its switching frequency so that its spectrum allows the generation of higher order harmonics. Class D PA implementation at high frequencies has been hindered for a long time as it exhibits low efficiency at high frequencies due to the large output shunt capacitance of the available power devices. However, the recently developed GaN HEMTs with a relatively low output drain capacitance can circumvent some of these problems. Generally, GaN HEMTs have a high power density, high break-down voltage, and low parasitic capacitances, making them an excellent candidate for high power and high efficiency applications. GaN HEMTs also have a very small value of on-state resistance ( $R_{on}$ ) when they function as switches that can lead to significant power loss reduction compared to other types of devices. Here a CREE GaN HEMT was selected to design a Class D PA. Table 1 shows the basic GaN HEMT compliance matrix and its compliance matrix selected for use. As shown in Table 1, CREE CGH40010F [14] is a good candidate to design a Class D PA.

**Table 1.** GaN performance in terms of device requirements for Class D PA.

	Device requirements of a Class D PA	GaN HEMT performance (CGH40010F) as example
High frequency switching	gain cut off frequency ( $f_T$ ) — the higher the better; usually about 10 times of the operating frequency	$f_T > 20$ GHz
High output power	breakdown voltage — the higher the better	$V_{br} > 84$ V
High efficiency	on-resistor — the smaller the better gain — the higher the better	$R_{on} = 1.1$ Ohm Gain $> 20$ dB @ 500 MHz
Low DC current consumption	drain current — the lower the better	$I_{dss} = 3.5$ A, usually less than 1 A
Wide band	small input/output/feedback capacitance	$C_{GS} = 4.5$ pF $C_{DS} = 1.3$ pF $C_{GD} = 0.2$ pF

#### 4. FILTER DESIGN

For a narrow band, Class D PA, serial or shunt output tank circuits are used to filter a sine wave output signal and reject all higher harmonics. Using a push-pull topology, the second harmonic signals are canceled in the output balun. However, for a wideband Class D PA in practice, the preferable output circuit is a set of switchable low pass filters instead of a series or a shunt harmonic termination. These output filters can be made by active or passive components. Although using an active filter can increase the output power, it also consumes more DC power and decreases the overall efficiency [12]. Therefore, passive filters have been adapted in this work. Here, four low pass filters (60 MHz/100 MHz/200 MHz/300 MHz) were designed to cover the 50 to 300 MHz range. However, for the frequency 300 to 550 MHz, the output transformer's cutoff performance can be used to reject the third harmonics at 900 to 1650 MHz. In this VHF/UHF band operation, lumped elements ( $L&C$ ) can still be used to design low pass filters, although the elements'  $Q$  is important in achieving a low insertion

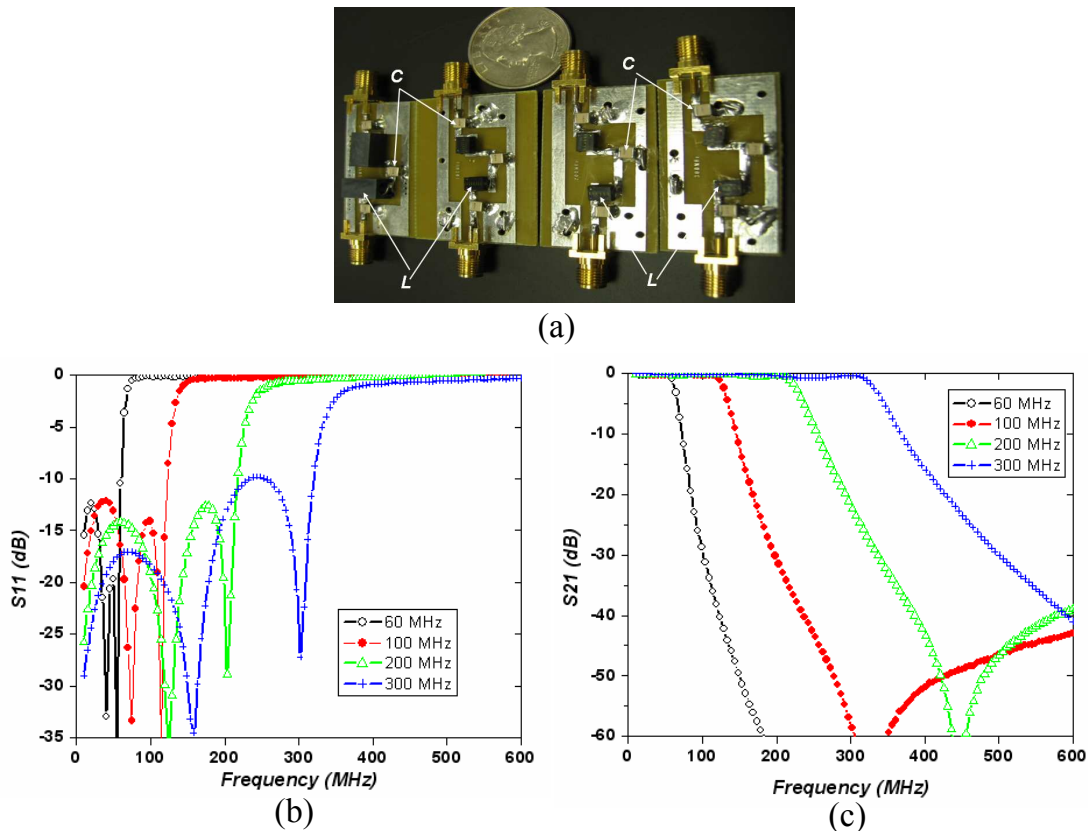


**Figure 3.** (a) Fabricated low pass filters; (b) Measured  $S_{11}$ ; (c) Measured  $S_{21}$ .

loss of the filter. Either the classic equations or the AWR Microwave Office can be used to synthesize a five-order Chebyshev low pass filter to adequately reject out-of-band signals. The order of the filters was compromised to the loss of the filter. Figure 3 shows the fabricated four low pass filters and their measured results. Each filter is a ladder network comprised of high  $Q$  ATC capacitors and air-core Coilcraft inductors mounted on a FR4 substrate. The fabricated filters have an insertion loss of about 0.25 dB and a good return loss over the required frequency range.

## 5. CIRCUIT SIMULATION AND IMPLEMENTATION

Generally, the zero voltage switching operation is preferred, since it can minimize energy dissipation and increase the power amplifier's drain efficiency. Additionally, the parasitic capacitances can be absorbed into the parallel output tank circuit for a high frequency operation. However, these advantages of CMCD are outweighed by various, serious disadvantages such as the required large inductor (RF choke) that would introduce an additional power loss and the use of a rectangular-wave drive that yields higher power losses in the gate circuit. Furthermore the loss due to switching the large rectangular currents using active devices would cause switching losses and may have additional saturation losses [13]. The theoretical comparison of VMCD and CMCD has been done in [15]. Either CMCD or VMCD has its own advantage. Some researchers designed CMCD at higher frequency ([8] & [9] as examples), since the parasitic capacitor of the device

**Table 2.** Current and voltage requirements for an ideal Class D power amplifier operation.

	VMCD	CMCD
$m/n$	$(1/2)^{0.5}$	$(2/3)^{0.5}$
$R = (m/n)^2 R_L$ $R_L = 50 \Omega$	$R = (1/2)50 = 25$	$50 * 2/3 = 33$
$V_{dd}$ (V)	28	28
$I_{dd}$ (A)	$I_{dd} = \frac{8}{\pi^2} \frac{V_{dd}}{R} = 0.91$	$I_{dd} = \frac{\pi^2}{8} \frac{V_{dd}}{R} = 1.05$
$V_{om}$ (V) peak voltage	$V_{om} = 2V_{dd} = 56$	$V_{om} = \pi V_{dd} = 88$
Output Power ( $> 20$ W for two device together)	$P_O = \frac{8}{\pi^2} \frac{V_{dd}^2}{R} = 25.4$	$P_O = \frac{\pi^2}{8} \frac{V_{dd}^2}{R} = 29.3$

can easily be absorbed into the shunt tank circuit. Some researcher designed VMCD for high power and high efficiency at lower frequency (Reference [12] as examples). Alternatively, the VMCD behaves like an ideal voltage source and whose output voltage is independent of the load. These factors indicate that it is a good candidate for linear amplification with nonlinear components (LINC) applications [16]. The design equations of VMCD and CMCD are given in [13] and are summarized in Table 2, which gives the output power, drain current, and drain voltage of an idealized operation of the Class D PA. The utilized GaN HEMT's breakdown voltage (84 V) is relatively high, allowing a trade-off of power for efficiency via the optimum choice of its resistive load ( $R_L$ ). Additionally, the 1:2 impedance transformer is much easier to implement than a (2/3) impedance transformer. Therefore, a VMCD topology has been selected for this study. Here, an initial value of  $R_L$ , has been determined as in the ideal VMCD topology. However, the optimal impedance load of the real device is still needed to achieve both high efficiency and high output power due to the parasitic of the device. For a more reliable and stable operation, the drain voltage ( $V_{dd}$ ) has been set at 28 V so that the peak drain voltage (56 V for VMCD) is more than 20% below its breakdown voltage (84 V).

A VMCD can be driven by either a rectangular-wave or a sine-wave signal. Obviously, a sine-wave drive is usually preferred since it takes less power and is much easier to generate. Meanwhile, the driver for the VMCD with HEMTs must produce a relatively large enough gate sinusoidal voltage to ensure a DC saturation and cutoff. Figure 4 shows the drain voltage of a GaN HEMT (as half of the VMCD) as a function of the input power. As shown here, the GaN HEMT should be driven into saturation ( $P_{in} = 25$  dBm) to operate as a switch and generate the desired symmetrical rectangular-wave voltage at the drain. However, an over-drive power ( $P_{in} = 30$  dBm) also causes

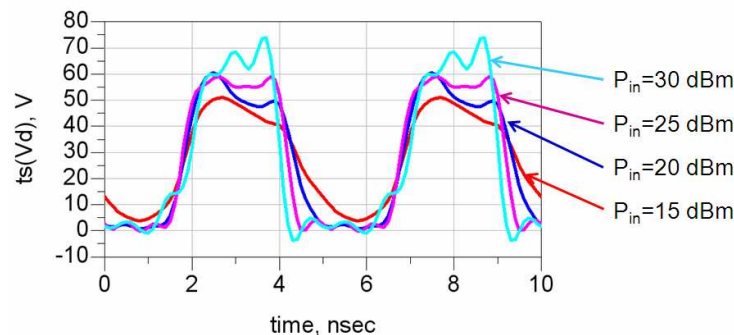


**Figure 4.** Transient drain voltage vs. input power.

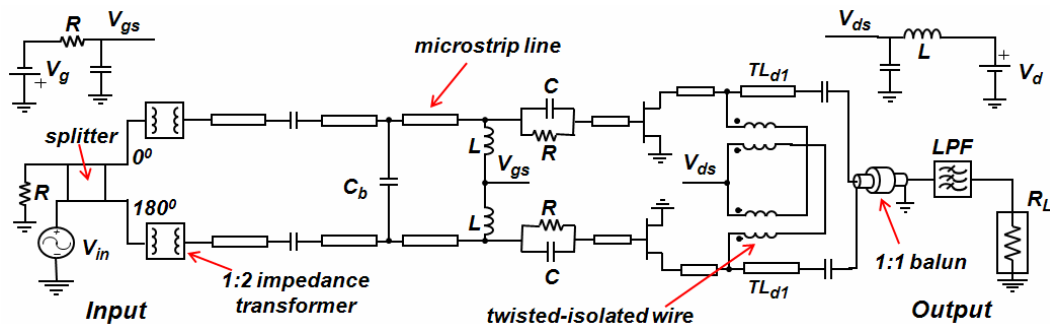


**Figure 5.** VMCD power amplifier simulation schematic.

an overshoot and an asymmetrical output voltage waveform.

The schematic of the designed wideband VMCD PA is shown in Figure 5. A simple bias network is used to achieve a voltage-mode operation. Two pairs of twisted-isolated wires are used to feed the devices' DC drain currents. The mutual inductive coupling coefficient between those twisted-isolated wires is critical in order to achieve a voltage-mode operation and to sustain high drain efficiency.

At the amplifier's input side, the signal is divided into two out-of-phase signals by a wideband 2-way 180° splitter. The out-of-phase signals are used to drive the GaN HEMTs in a push-pull configuration and their levels were 25 dBm. It was also predicted based on the large signal analysis that the optimum input impedance of the device is about 25  $\Omega$  over 50 to 550 MHz. Subsequently, a wideband 1:2 impedance transformer is required at the input section of each device to transform 50  $\Omega$  to 25  $\Omega$  to sustain a good input match. However, a 1:2.25 impedance transformer was used instead for ease of its implementation based on Sevick's work [17]. Additionally, a small shunt capacitor ( $C_b$ ) was connected between the two input branches and was used as a bridge to improve the balance between those two inputs.

At the amplifier's output side, the  $R_{on}$  of the CGH40010F is around 1.1  $\Omega$ , which is a small impedance and excellent for high efficiency operation. Meanwhile, the optimum load impedance for high drain efficiency can be estimated using either the simplified equations (shown in Table 2) or more accurate load-pull simulations. In this case, the rough estimate is  $R = 25 \Omega$  for a 25 W output power with a 28 V drain voltage. Large signal analysis has been applied for optimum load simulation. The equivalent optimum load ( $R_p$ ) of the single GaN HEMT turned out to be quite close to the estimated  $R$  value over wideband as shown in Table 3 (operates close to the pinch-off bias to achieve about 42 dBm output power and a high efficiency exceeding



**Table 3.** Load-pull simulation results with 25 dBm input power and  $25\ \Omega$  input impedance.

Freq (MHz)	Pout (dBm)	PAE (%)	$R_p$ ( $\Omega$ )	$C_p$ (pF)
50	43.8	76.5	24.8	10.9
100	43.5	74.5	24.8	5.5
150	43.2	72.5	24.8	3.7
200	42.4	75.1	33.1	1.9
250	42.2	72.6	33.1	1.5
300	41.9	70.0	33.1	1.3
350	42.2	70.3	33.0	9.9
400	42.3	73.3	27.0	5.6
450	42.3	73.6	27.0	5.0
500	42.2	73.4	27.0	4.5
550	42.0	73.2	27.0	4.1

70% over wideband). Also the width and length of microstrip line ( $TL_{d1}$ ) are tuned for better wideband performance. Subsequently, two out-of-phase drain signals are combined into one output signal using a 1:1 balun. This balun is used as a combiner and impedance transformer ( $25\ \Omega$  to  $50\ \Omega$ ) as well, and its design is based on a Multi-hole ferrite core ( $\mu_r = 125$ ) and a coaxial line ( $50\ \Omega$ ). Using a push-pull topology, the second harmonic signals are typically cancelled in the output balun. A bank of low pass filters is utilized on the output side of the 1:1 balun to reject the third harmonic of the rectangular waveform.

The design/optimization of the PA has been carried out in Agilent's Advanced Design System. In this nonlinear analysis, it is preferable to use the fine tuning tool rather than using an automatic optimization to avoid convergence problems. Figure 6(a) shows the simulation results of the wideband VMCD PA, where the output power and drain efficiency are higher than 44.2 dBm and 64% over 50 to 550 MHz, respectively with an input power of 28 dBm. As shown in Figure 6(b), the drain voltage is a slightly distorted rectangular waveform with 56 V peak value and its current is a slightly distorted half sine wave. This distortion is due to the parasitic nature of the device. Although for a narrow band VMCD PA the distortion can be minimized by fine tuning the matching network, for a wideband VMCD PA this distortion has to be traded off for output power and high efficiency over frequencies.

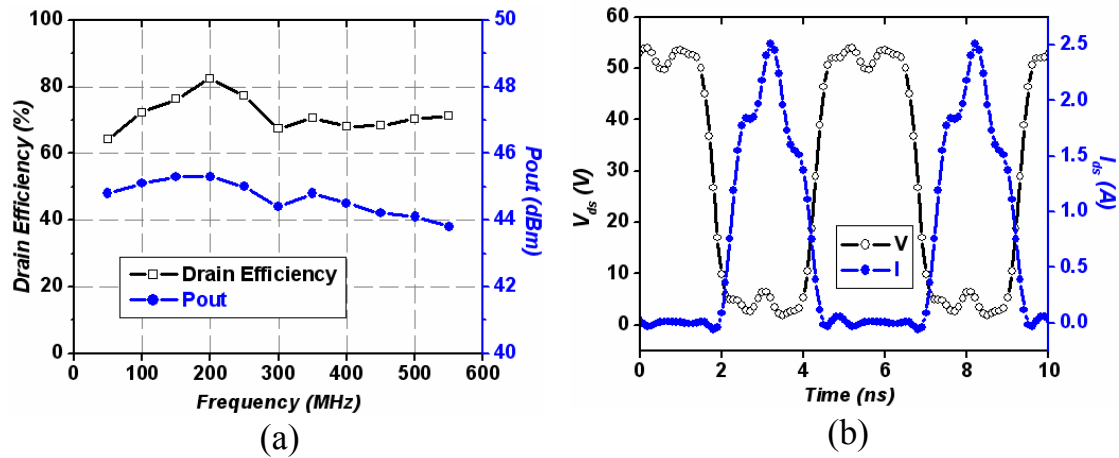


**Figure 6.** (a) Simulated drain efficiency & output power; (b) Simulated transient waveform at 200 MHz.

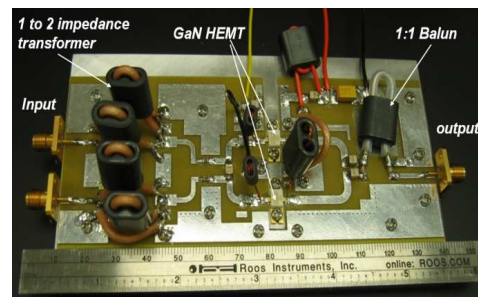


**Figure 7.** Fabricated VMCD PA.

## 6. EXPERIMENTAL CIRCUITS AND RESULTS

The designed VMCD PA was built on a FR4 substrate with a dielectric constant of 4.4 and a thickness of 1.57 mm. The fabricated circuit is shown in Figure 7. For testing purposes here, four low pass filters (as shown in Figure 3(a)) are used to manually cover the 50 to 300 MHz range. However, for the frequency 300 to 550 MHz, it is adequate to use the cutoff performance of the output transformer to reject the third harmonic at 900 to 1650 MHz. Meanwhile, to have a proper mode of operation of the active devices, the input power level was sustained at 25 dBm by using a 28.5 dBm driver amplifier; as the input 2-way splitter has about 0.5 dB insertion loss. The highest measured drain efficiency was achieved when the PA was biased close to its pinch-off, consistent with the simulation results. Figure 8(a) depicts that the measured output voltage is almost a linear function of the drain voltage  $V_{dd}$ , when keeping the input power fixed. Figure 8(b) shows both the drain efficiency and output power of the fabricated VMCD PA over frequencies. It was also found that by adding a bead ferrite

core ( $\mu_r = 125$ ) to the twisted-isolated wires used for DC biasing would improve the low frequency drain efficiency. Additionally, the measured gain of this PA is higher than 14.5 dB over the operating frequency range. The measured drain efficiency exceeded 63%; however, these results will be slightly degraded if the filter loss of 0.25 dB is taken into account. Here, a bank of low pass filters was utilized to suppress the third harmonic, which could also be replaced by a reconfigurable filter for automatic operation.

The GaN devices, as usual, have a soft power compression characteristic which could reduce linearity. At the same time, the SMPA operation requires significant gain compression to generate higher harmonics. One important measure of linearity, IMD, is usually measured using a two-tone signal. As expected, this VMCD PA has poor linearity: at an input power of 28 dBm (199 MHz and 201 MHz), the IMD3 is around 12 dBc, while the IMD5 is approximately 23 dBc. However, the linearity of the VMCD PA can also be characterized by considering the drain bias as the input signal [18]. In this context, the AM-AM conversion is measured as the increase in output voltage (with a  $50\ \Omega$  load) when the drain bias is increased linearly. For high input power, the VMCD PA's output voltage varies linearly with drain voltage, as shown in Figure 8(a). And when the input power is decreased, the VMCD PA's AM-AM characteristics are no longer linear. Therefore, applications of Class D amplifiers that require high linearity should utilize EER or LINC subsystems for external linearization [1].

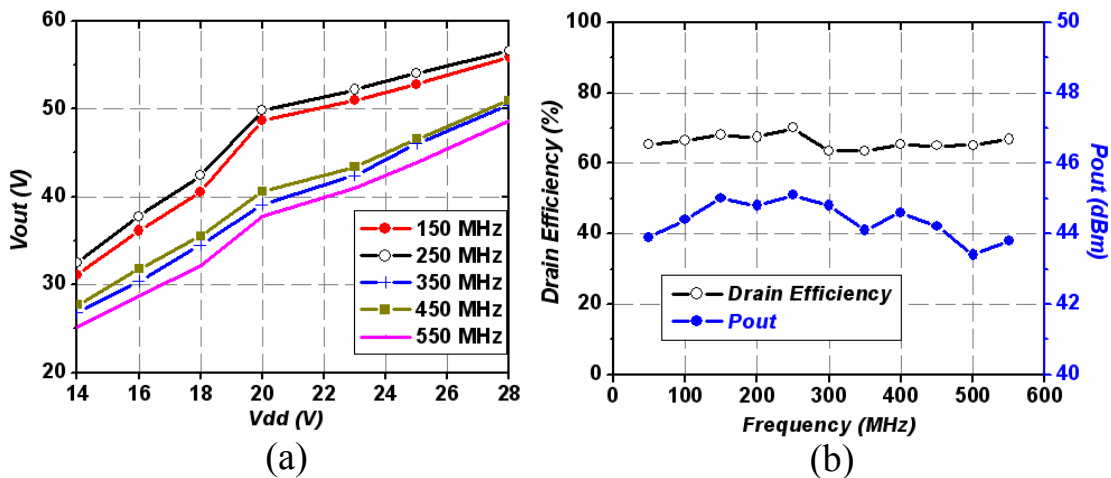


**Figure 8.** (a) Variation of the measured output voltage as a function of drain voltage; (b) Measured output power and drain efficiency.

## 7. CONCLUSION

A VHF/UHF high power wideband VMCD PA using GaN HEMTs was simulated, fabricated, and tested. The measured drain efficiency was in the range of 63% to 72% over a wide frequency (50 to 550 MHz) with an output power from 43 to 45 dBm. Generally, the GaN HEMT's very small value  $R_{on}$  helps to lower the power loss. The GaN HEMT's small parasitic drain to source capacitance ( $C_{ds}$ ) results in higher drain efficiency and a larger bandwidth when compared to other device technologies, such as Si LDMOS. It is possible to obtain a greatly increased performance in both drain efficiency and output power for narrow band applications. However, to achieve a wideband operation, the drain efficiency and output power need to be compromised. Finally, from an insertion loss perspective, using a wideband reconfigurable filter rather than a filter bank may be a better solution for overall high efficiency.

## REFERENCES

1. Raab, F. H., P. Asbeck, S. Cripps, P. B. Kenington, Z. B. Popovic, N. Pothecary, J. F. Sevic, and N. O. Sokal, "Power amplifiers and transmitters for RF and microwave," *IEEE Trans. Microw. Theory Tech.*, Vol. 50, 814–826, 2002.
2. Jimenez Martin, J. L., V. Gonzalez-Posadas, J. E. Gonzalez-Garcia, F. J. Arques-Orobon, L. E. Garcia Munoz, and D. Segovia-Vargas, "Dual band high efficiency class ce power amplifier based on CRLH diplexer," *Progress In Electromagnetics Research*, Vol. 97, 217–240, 2009.
3. Chung, Y., S. Cai, W. Lee, Y. Lin, C. P. Wen, K. L. Wang, and T. Itoh, "High power wideband AlGaIn/GaN HEMT feedback amplifier module with drain and feedback loop inductances," *Electronics Letters*, Vol. 37, 1199–1200, 2001.
4. Jong-Wook, L. and K. J. Webb, "Broadband GaN HEMT push-pull microwave power amplifier," *IEEE Microwave and Wireless Components Letters*, Vol. 11, 367–369, 2001.
5. Lin, S., M. Eron, and A. E. Fathy, "Development of ultra wideband, high efficiency, distributed power amplifiers using discrete GaN HEMTs," *IET Circuits, Devices & Systems*, Vol. 3, 135–142, 2009.
6. Yi, H. and S.-Y. Hong, "Design of L-band high speed pulsed power amplifier using ldmos fet," *Progress In Electromagnetics Research M*, Vol. 2, 153–165, 2008.

7. Baxandall, P. J., "Transistor sinewave oscillators," *IEE Proc.*, 748–758, London, May 1959.
8. Ji-Yeon, K., H. Dong-Hoon, K. Jong-Heon, and S. P. Stapleton, "A 50 W LDMOS current mode 1800 MHz class-D power amplifier," *IEEE MTT-S*, 1295–1298, 2005.
9. Nemati, H., "Design, implementation and evaluation of a current-mode class-D power amplifier," Master's Thesis, Chalmers University of Technology, 2006.
10. Kobayashi, H., J. M. Hinrichs, and P. M. Asbeck, "Current-mode class-D power amplifiers for high-efficiency RF applications," *IEEE Trans. MTT*, Vol. 49, 2480–2485, 2001.
11. Gustavsson, U., "Design of an inverse class D amplifier using GaN-HEMT technology," MSc, Örebro University, 2006.
12. Hegazi, G., T. Chu, S. Heibel, J. Jordan, and H. Sasmazer, "Linear wideband VHF/UHF quad LINC transmitter system," *IEEE Military Communications Conference, MILCOM 2007*, 1–6, 2007.
13. Grebennikov, A. and N. O. Sokal, *Switch Mode RF Power Amplifiers*, Newnes, 2008.
14. CGH40010F/CGH60015D Datasheet, Cree Inc..
15. Albulet, M., *RF Power Amplifiers*, Noble Publishing Associates, Jan. 2001.
16. Yao, J. and S. I. Long, "Power amplifier selection for LINC applications," *IEEE Trans. on Circuits and Systems II: Express Briefs*, Vol. 53, No. 8, 763–767, 2006.
17. Sevick, J., *Transmission Line Transformer*, Noble Publishing, Atlanta, 2001.
18. Wang, N., X. Peng, V. Yousefzadeh, D. Maksimovic, S. Pajic, and Z. Popovic, "Linearity of X-band class-E power amplifier in EER operation," *IEEE Trans. Microw. Theory Tech.*, Vol. 53, 1096–1102, 2005.